INSTITUT DE FRANCE
Académie des sciences

Comptes Rendus

Géoscience

Sciences de la Planète

Carlo Mologni, Marie Revel, Luc Bastian, Germain Bayon, Delphine Bosch, Lamya Khalidi and Nathalie Vigier

Enhanced continental weathering (δ^7Li, εNd) during the rise of East African complex polities: an early large-scale anthropogenic forcing?

Volume 354 (2022), p. 319-337

Published online: 3 November 2022

https://doi.org/10.5802/crgeos.169

Les Comptes Rendus. Géoscience — Sciences de la Planète *sont membres du Centre Mersenne pour l'édition scientifique ouverte*
www.centre-mersenne.org
e-ISSN : 1778-7025

Comptes Rendus
Géoscience — Sciences de la Planète
2022, Vol. 354, p. 319-337
https://doi.org/10.5802/crgeos.169

Original Article — Geochemistry, cosmochemistry

Enhanced continental weathering (δ^7Li, εNd) during the rise of East African complex polities: an early large-scale anthropogenic forcing?

Carlo Mologni *, [a, b], **Marie Revel** [a], **Luc Bastian** [a, c], **Germain Bayon** [d], **Delphine Bosch** [e], **Lamya Khalidi** [b] and **Nathalie Vigier** [c]

[a] Univ. Côte d'Azur, CNRS, OCA, IRD, Geoazur, 250 rue Albert Einstein, 06500 Valbonne, France

[b] Univ. Côte d'Azur, CNRS, CEPAM – UMR 7264, 24 av. des Diables Bleus 06300 Nice, France

[c] Laboratoire d'Océanographie de Villefranche sur Mer (LOV, IMEV), CNRS, Sorbonne Université, 181 chemin du Lazaret, 06320, Villefranche sur Mer, France

[d] IFREMER, Unité de Recherche Géosciences Marines, 29280 Plouzané, France

[e] Géosciences Montpellier, UMR-CNRS 5243, Université de Montpellier, 34095 Montpellier, France

E-mails: mologni@geoazur.unice.fr, mologni@cepam.cnrs.fr (C. Mologni), revel@geoazur.unice.fr (M. Revel), 3bastianl@gmail.com (L. Bastian), Germain.Bayon@ifremer.fr (G. Bayon), delphine.bosch@umontpellier.fr (D. Bosch), Lamya.KHALIDI@cepam.cnrs.fr (L. Khalidi), nathalie.vigier@imev-mer.fr (N. Vigier)

Abstract. Human-induced environmental disturbances during the Holocene have provided support for the Early Anthropogenic Hypothesis (EAH), which proposes that with the advent of agro-pastoralism and associated deforestation, humans have modified CO_2 and CH_4 concentrations into the atmosphere. However, only limited evidence exists for human driven chemical alteration of the Earth's Critical Zone (ECZ) in early antiquity. Here, we explore the impact of human activities on both erosion and chemical weathering patterns in the Nile basin during a time interval that includes the rise of the Aksumite Kingdom and Late Antique Egypt (~3–~1 ka BP). By coupling lithium and neodymium isotopes (δ^7Li, εNd) in clay-size fractions of two marine sediment cores from the Nile Deep Sea Fan (NDSF), we reconstruct the variability of sediment provenance and silicate weathering intensity in the Nile basin over the last 9000 years. Our high temporal resolution data show that for the last ~3000 years, the Rosetta Nile Deep Sea Fan has been increasingly fed with clays delivered from the Ethiopian basaltic highlands (εNd = ~−1), despite the absence of hydrological intensification and major climatic drivers over that region. Concomitantly, the clay Li isotopic composition shifted towards lower δ^7Li values (δ^7Li = 1 to −2), yielding unprecedented negative values for at least the last 100,000 years. Combined with other archaeological, paleo-pedological and organic chemistry inferences, the Li–Nd isotope proxy records indicate a link between the intensification of continental weathering and intensified land-use and water management during the Pre-Aksumite (~3 to ~2 ka BP) and Aksumite (~2 to

* Corresponding author.

~1 ka BP) periods. Therefore, our results provide direct support to the hypothesis of an early and large scale anthropogenic forcing on continental chemical weathering. A comparison with previously published records for Central Africa, Central Europe and China suggests that the impact of the intensification of early agriculture on the ECZ may have operated at a global scale starting around four thousand years ago.

Keywords. Chemical weathering, Li isotope, Nd isotope, Nile deep sea fan, Anthropogenic forcing, Aksumite civilization, Earth Critical Zone.

Note. Submission by invitation of the editorial board.

Manuscript received 31 May 2022, revised 30 September 2022, accepted 3 October 2022.

1. Introduction

The Early Anthropogenic Hypothesis (EAH) considers that human activities related to early agriculture, herding and deforestation may have played a crucial role in driving the onset of global warming between 7 and 5 ka BP, as inferred from the increase of atmospheric CO_2 and CH_4 emissions recorded in high-latitude ice cores [Ruddiman, 2003, Ruddiman et al., 2020]. However, the impact of human activities on landscapes, and how they affected the Earth Critical Zone [ECZ; Lin, 2009] since prehistoric times, remains poorly documented. Recently, a number of geochemical proxies of past continental chemical weathering have emerged. These have great potential to provide key information on the ECZ dynamics. Among them, Li isotopes have been successfully applied to fine-grained sediment records of river-borne particles exported to deltas, alluvial terraces and lakes [Bastian et al., 2017, Rothacker et al., 2018, Yang et al., 2021]. A covariation of Li isotopic compositions with various climate proxies during the Quaternary period has demonstrated the rapid response of soil/rock weathering to major precipitation changes, in particular during arid/humid precessional cycles in the tropics and during glacial/interglacial cycles at higher latitudes [Bastian et al., 2019, 2017, Yang et al., 2021, Rothacker et al., 2018, Dosseto et al., 2015]. In soils, the lightest lithium isotope (^{6}Li) is preferentially incorporated into secondary clay mineral phases as a result of mass-dependent isotope fractionation occurring during mineral/water interactions [Hindshaw et al., 2018, Vigier et al., 2008]. The δ^7Li values of clay minerals can reflect the degree of continental weathering expressed as the ratio between dissolution rate of primary minerals versus clay neoformation rates [Bastian & Mologni et al., 2021, Pogge von Strandmann et al., 2017, 2020, Vigier et al., 2009]. In large continental-scale basins, where chemical and physical erosion operate under steady-state conditions, this ratio can be related to the intensity of chemical weathering, expressed as the ratio of silicate chemical weathering over total denudation [W/D ratio; Bouchez et al., 2013, Caves Rugenstein et al., 2019, Dellinger et al., 2017]. The provenance of fine-grained sediment in the Nile delta can be identified through its neodymium isotopic signature (εNd) [Bastian & Mologni et al., 2021, Blanchet, 2019, Blanchet et al., 2014, Revel et al., 2015, Weldeab et al., 2014]. As no significant fractionation is observed during chemical weathering, εNd reflects the isotopic composition of the parent bedrock and the origin of the material. Since the Nile basin encompasses the Precambrian African basement as well as the Ethiopian and Somalian Cenozoic basalts, which have contrasting isotopic compositions, the Nd isotopic composition of sediment loads is suitable to distinguish their source regions [Bayon et al., 2015, Blanchet, 2019, Grousset et al., 1988]. Our approach combines the use of neodymium and lithium isotope proxy records, together with measured sedimentation rates, in order to provide constraints on past hydrological conditions, sediment transport, and chemical weathering intensity in the Nile River watershed.

Major hydro-climate variability related to changes in insolation and monsoon dynamics were observed over tropical Africa during the Quaternary period, during which time ~21 ka cycles of intense humid periods alternated with arid periods [Blanchet, 2019, Blanchet et al., 2021, Kutzbach et al., 2020, McGee and deMenocal, 2017, Ménot et al., 2020, Pausata et al., 2020]. This variability has been documented in several high-temporal resolution marine sediment records retrieved from the Nile Deep Sea Fan [NDSF; Bastian & Mologni et al., 2021, Bastian et al., 2017, Blanchet et al., 2015, Ménot et al., 2020, Mologni et al., 2020, Revel et al., 2015].

Between ~3 and ~1 ka BP, the Nile River Basin was home to Pre-Aksumite cultures followed by the

Aksumite Kingdom, known to be one of the most important ancient East African civilizations [Anfray, 1967, Fattovich, 2010, Gerlach, 2015, Japp, 2019, Phillipson, 2012]. Ancient Egyptian civilization was established further northward along the Nile mainstream and delta, and its emergence as early as 5000 cal. years BP has been associated with changes in the annual cycle of the Nile summer floods [e.g. Manning et al., 2017, Sheisha et al., 2022] suggesting a relationship between the end of the African Humid Period (AHP) and the Protodynastic period in Egypt.

The Aksumite kingdom was mostly located in the Ethiopian highlands, an area almost exclusively composed of Cenozoic basaltic rocks (Ethiopian Traps), Mesozoic sediments underlain by the Pan-African basement (Figure 1b). The Ethiopian Traps are characterized by a radiogenic neodymium (Nd) isotopic signature with an εNd ranging between ~0–~7 [Garzanti et al., 2015], which differs largely from the εNd composition of the detrital sediment derived from other branches of the Nile catchment (Figure 1a). As a consequence, the Nd isotopic composition of the fine-grained sediment deposited at the NDSF can be used to identify the contribution of river-borne particles transported by the Blue Nile and the Atbara/Tekeze headwaters. These drain the Ethiopian Highlands which were occupied by the territories of the Pre-Aksumites and Aksumite Kingdom, as well as the White Nile branch (draining the Central African Craton), and those derived from aeolian inputs from the nearby Saharan Metacraton [Mologni et al., 2020, Bastian et al., 2017, Blanchet et al., 2013, Revel et al., 2015]. Previous studies on the combined use of lithium and neodymium isotopes in clay-size fractions of sediment deposited in the NDSF indicated a close relationship between hydrological changes, continental chemical weathering and the delivery of material derived from the Ethiopian Traps over the past 100 to 1 ka [Bastian & Mologni et al., 2021]. In this study, we reconstruct the variability of sediment provenance and chemical weathering in the Nile Basin using a marine sediment record covering the last 9000 years. This record cover to the period associated with the rise of the first East African complex polities, namely the Pre-Aksumite cultures (~3 to ~2 ka BP) and the Aksumite Kingdom (~2 to ~1 ka BP) that proceeded it [Fattovich, 2010, Phillipson, 2012], which are contemporaneous with the Ancient Egyptian Dynastic, Ptolemaic and Roman civilizations [Manning et al., 2017]. In addition to discussing original data on marine sediments, we use a wealth of information provided by a number of Holocene paleo-pedological [Bard et al., 2000, Gebru et al., 2009, Terwilliger et al., 2013, 2011], archaeological and paleoclimatic [Costa et al., 2014, Jaeschke et al., 2020] investigations conducted in the Ethiopian Highlands to discuss potential impacts of intensified land-use by Aksumite and Late Egyptian complex polities on sediment transport and chemical weathering intensity.

2. Materials and methods

The Nile Delta deep sea cores we sampled display irregular shoreline protuberances directly under the influence of the Nile River's hydro-sedimentary activity [Mologni et al., 2020]. A substantial fraction of the fine-grained particulate load delivered from the Nile River is stored on the Egyptian continental slope in the form of mixed deposits of fine-grained turbidites and hemipelagic sediments. In this study, we investigate two well-dated sediment sequences: core MS27PT [N31° 47.90′; E29° 27.70′; 1389 m water depth; Bastian & Mologni et al., 2021] and core MD04-2726 [N31° 51.00′; E29°47.49′; 1058 m water depth; Mologni et al., 2020], which provide a continuous record of clastic particles exported from the Nile river basin over the last ~100 ka and 11 ka, respectively. The age models of these sediment records are based on 59 previously published radiocarbon dates [Bastian & Mologni et al., 2021, Mologni et al., 2020, Revel et al., 2015, 2010]. In this study, we present new results obtained from the upper 2 m of MD04-2726, focusing on the finest (<2 μm) clay-size detrital fraction. Because the clay-size fractions deposited near the mouth of rivers include secondary clay minerals initially formed in soil weathering profiles, they are thus well suited for the investigation of past silicate chemical weathering in river catchments. Additionally, due to their small size and density, clays are expected to be efficiently delivered from source to sink [Bastian et al., 2017].

2.1. *Lithium isotope analyses*

Chemical purification of Li was performed at the LOV (Laboratoire Océanographique de Villefranche-sur-Mer) in a clean laboratory. A solution containing

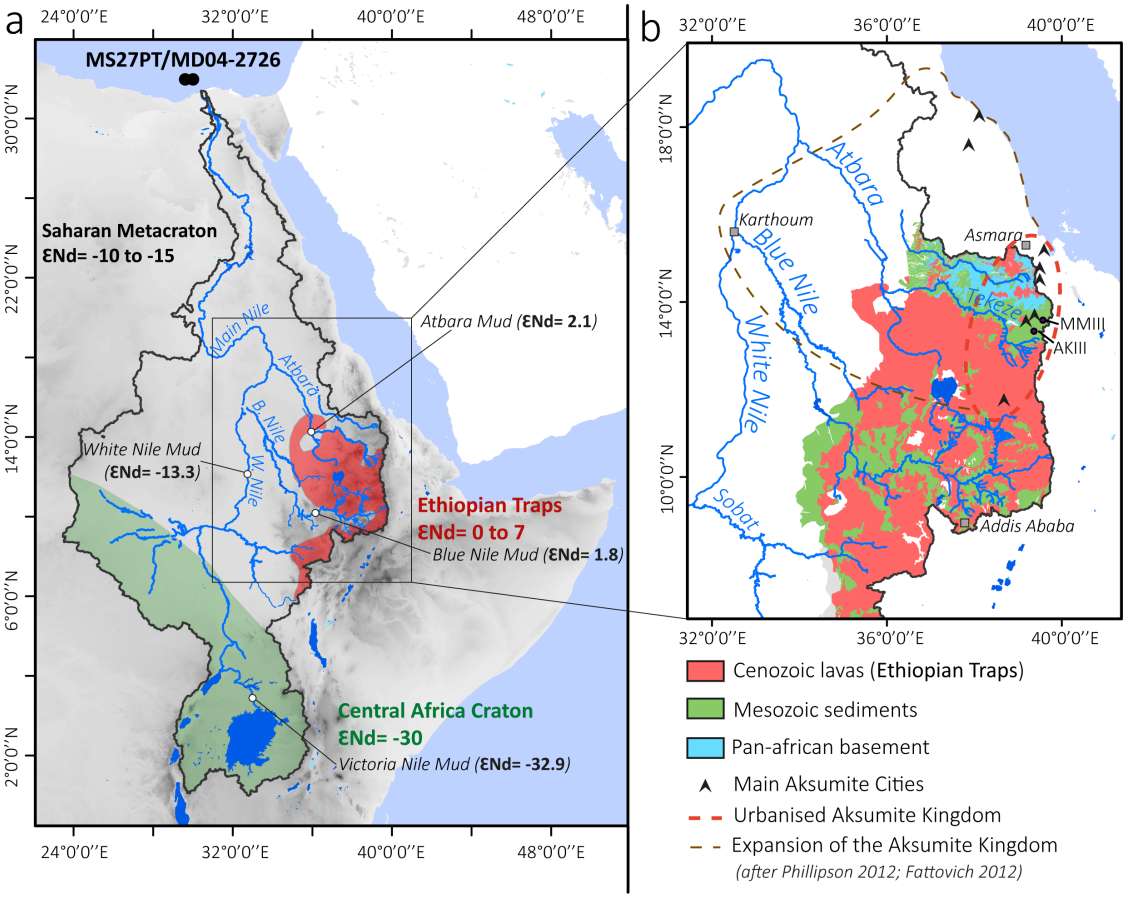

Figure 1. (a) Map of the Nile River basin and location of cores MS27PT (N31° 47.90′; E29° 27.70′, 1389 m water depth) and MD04-2726 (31° 51.000′ N, 29° 47.490′ E, 1058 m water depth) in the NDSF. Three main sources of sediment are identified in the Nile basin: the basaltic rocks (red) of the Ethiopian traps (Highlands), which are drained by the Blue Nile, the Atbara/Tekeze and Sobat rivers located in tropical latitudes (around 5 to 15° N); the Precambrian metamorphic rocks (green) of the Central African Craton located in the Ugandan headwaters region of the White Nile and drained by the Bahr el Jebel River; and the Saharan Metacraton sources [Abdelsalam et al., 2002, Grousset and Biscaye, 2005, Scheuvens et al., 2013]. εNd values for the Victoria, White and Blue Nile River mud samples are from Garzanti et al. [2015]. (b) Map of the Blue Nile and Atbara River basins with the location of the main Aksumite cities [black triangles, after Fattovich, 2010, Phillipson, 2012], modern towns (grey squares), the limits of the Nile river catchment (black line), the urbanized Aksumite territories (red dotted line), the expansion of the Aksumite kingdom [brown dotted line; after Fattovich, 2010, Phillipson, 2012], Mai Maikden (MMIII, brown circle) and Adi Kolen (AKIII, green circle) soil sequence studies presented in Figure 3 [Gebru et al., 2009, Terwilliger et al., 2011, 2013].

~60 ng of lithium was introduced on a cationic resin column (AG50X12) and Li was eluted using titrated ultrapure 1.0 N HCl [Vigier et al., 2008]. This separation was performed twice to ensure perfect Li–Na separation. LiCl solution was then evaporated to dryness and re-dissolved in 0.05 N HNO_3 for isotope analyses. Lithium isotope analyses ($\delta^7Li = ((7Li/6Li)/(7Li/6Li)LSVEC - 1) \times 1000$, LSVEC being the international standard) were performed at the Ecole Normale Supérieure de Lyon (CNRS-INSU

National Facilities) using a Neptune *Plus* (Thermo-Fisher) multi-collector inductively coupled plasma spectrometer (MC-ICP-MS) along with a sample-standard bracketing technique. A combination of Jet and X cones were used, as well as an Aridus II desolvating system, resulting in a sensitivity of 1 V ^{7}Li/ppb [Balter and Vigier, 2014, Thibon et al., 2021]. Before analyses, Li fractions were diluted to match 4 ppb Li. Total procedural blanks were negligible (<10 pg Li), representing ~0.02% maximum of the total Li fraction for each sample. The accuracy of isotopic measurements was assessed several times during each measurement session using reference Li^7–N solution [Carignan et al., 2007] and other reference materials [BE-N and JB-2 rocks and seawater, see Verney-Carron et al., 2015].

2.2. *Neodymium isotope analyses*

Neodymium isotopic ratios were measured at the Pôle Spectrométrie Océan (Brest, France). For convenience, Nd isotopic ratios results are expressed as: $\varepsilon Nd = [[^{143}Nd/^{144}Nd(meas.)/^{143}Nd/^{144}Nd(CHUR)] - 1] \times 10^4$. The CHUR (Chondritic Uniform Reservoir) value is 0.512638 [Jacobsen and Wasserburg, 1980]. Neodymium was purified using conventional ion chromatography [Bayon et al., 2012]. Nd isotopic compositions were determined using sample-standard bracketing by analysing JNdi-1 standard solutions every two samples. Mass bias corrections were made using the exponential law considering $^{146}Nd/^{144}Nd = 0.7219$. Mass-bias corrected values for $^{143}Nd/^{144}Nd$ were normalized to a JNdi-1 value of $^{143}Nd/^{144}Nd = 0.512115$ [Tanaka et al., 2000]. Repeated analyses of bracketed JNdi-1 standard solutions during the course of this study yielded $^{143}Nd/^{144}Nd$ of 0.512117 ± 0.000012 (2 SD, $n = 38$), corresponding to an external reproducibility of $\sim \pm 0.23\varepsilon$ (2 SD).

3. Results: Li and Nd isotopic compositions of clay fractions

Bastian & Mologni et al. [2021] show how the Nd isotopic composition of clay-size fractions from core MS27PT varies from $\varepsilon Nd < -3$ during humid periods to −8 during arid periods, following the variability of insolation between precession maxima and minima periods between 100 and 3 cal. ka BP (Figure 2).

Our new results show that the εNd values of clays separated from core MD04-2726 vary between −2.3 to −6 at the end of the AHP (Table 1). This range of εNd values is similar to one observed in the core MS27PT over the last 100 ka insolation cycles. Surprisingly, after 2.3 ka, the Nd isotopic composition of clay-size fractions from both cores increases gradually but significantly, to reach a maximum radiogenic εNd value of −1 around 400 years ago.

The δ^7Li composition of clays from core MS27PT varies between 4‰ and 1‰ during the last 100 ka (Table 2), following the alternation between insolation minima and maxima periods. As for Nd isotopes, after 3 ka, clay δ^7Li reached values that are unprecedented in the last 100 ka, and it decreased gradually, to reach a value of −2.5‰ 400 years ago.

4. Discussion

4.1. *Evidence for non-climatic forcing on chemical weathering since 3000 years cal. BP*

A striking result of our study is that since 3000 cal. years BP, the Li isotopic composition of clay-size fractions has decreased to negative values, differing substantially from the observed δ^7Li trend observed over the last 100 cal. ka BP [Figure 2; Bastian & Mologni et al., 2021]. This observation implies (1) that a new forcing gradually appeared around ~3000 cal. BP, resulting in an increase in the intensity of chemical weathering, and (2) that this forcing dominated other controlling factors that were at play before, namely those related to insolation-driven hydro-climate variability and ocean dynamics [see e.g. Bastian & Mologni et al., 2021].

Estuarine and deltaic processes may contribute to an *in situ* weathering of primary minerals deposited in the NDSF [Zhang et al., 2022a,b]. However, it has been demonstrated by Bastian et al. [2017] that variations in δ^7Li recorded in the NDSF clay fraction cannot be explained by diagenetic processes. Early clay diagenesis and seawater isotopic fractionation is normally characterised by higher δ^7Li than continental weathering products [Wei et al., 2020], which can even be associated with Li absorption from seawater [δ^7Li = 31.2; Misra and Froelich, 2012]. More negative δ^7Li recorded at the top of the core allow us to exclude this effect for the NDSF. Indeed, small quantity of organics in sediments could

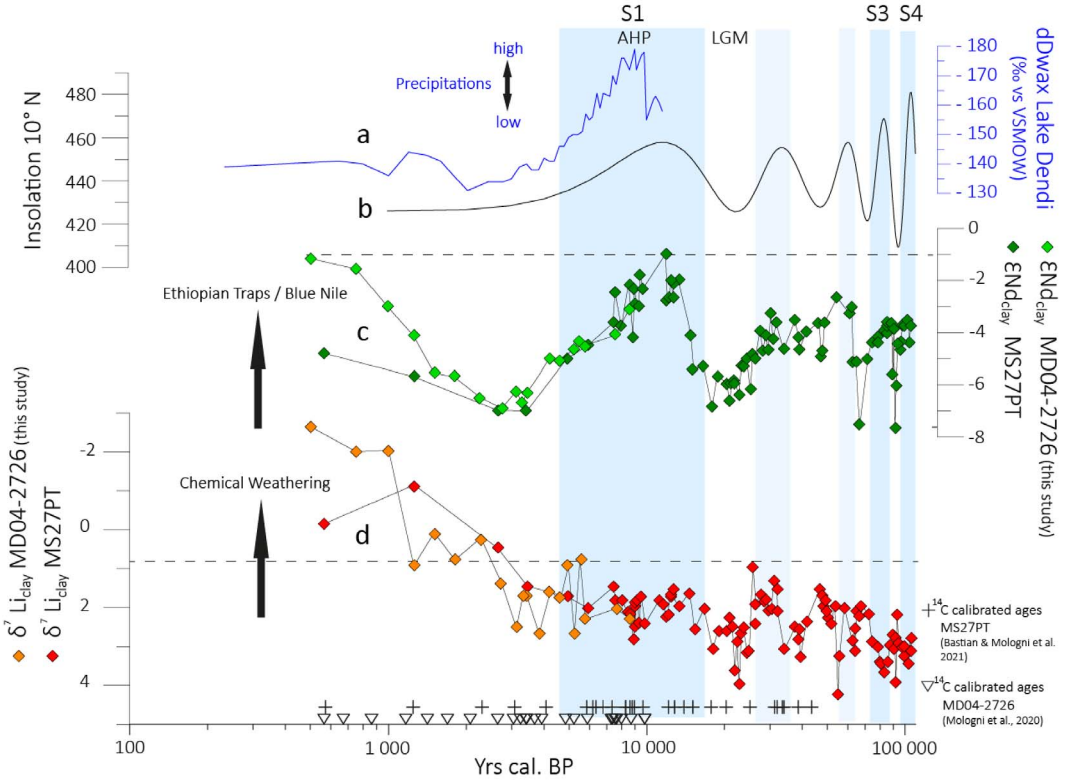

Figure 2. A selection of paleoenvironmental proxy records for East Africa. (a) δD_{wax} of Lake Dendi [Jaeschke et al., 2020]; (b) July insolation in watt/m^2 at 10° N [Berger and Loutre, 1991]; (c) εNd values of clay-size fractions of cores MS27PT (dark green points) and MD04-2726 (light green points) cores; (d) δ^7Li values of clay-size fractions of cores MS27PT (red points) and MD04-2726 (orange points) cores. Black crosses and reversed triangles indicate ^{14}C calibrated ages of MS27PT and MD04-2726 cores respectively. S1, S3 and S4 refer to Sapropel 1, 3 and 4 respectively; AHP refers to "African Humid Period" and LGM to "Last Glacial Maximum" period.

favour the stabilization of deposited primary phases [Krissansen-Totton and Catling, 2017, Michalopoulos and Aller, 2004].

The provenance of clays transported by the Nile River can be inferred from Nd isotopes. The clay-size fractions deposited during the last 3000 years at sites MD04-2726 and MS27PT display a trend towards markedly increasing εNd values similar to the highly radiogenic values typical of the Ethiopian Traps that are generally encountered during past African Humid Periods. The same trend towards more radiogenic values (up to εNd ~ 0.4) is also recorded for the last 1880-year interval of core P362/2-33, a nearby marine sediment core retrieved from the NDSF Rosetta system [Blanchet et al., 2015, 2013]. Over the last 100 ka, the time intervals corresponding to the deposition of clays with radiogenic (high) εNd signatures were systematically associated with an increase in sedimentation rates (up to ~100 cm/ka), best explained by higher physical erosion rates in the Ethiopian Traps area [Bastian & Mologni et al., 2021, Revel et al., 2010]. In contrast, since 3000 years cal. BP, the observed increase in εNd values has been associated with relatively low sedimentation rates [>2 cm/ka; Revel et al., 2015] and low terrigenous fluxes [<4 g/cm^2/ka; Revel et al., 2014], in agreement with lower insolation and precipitation patterns (Figure 2). As previously shown in Bastian & Mologni et al. [2021] and Mologni et al. [2020], this may result from low fluvial transport of fine-grained sediments still active during arid climates, since more that 80% of the sediment deposited at the NDSF originates

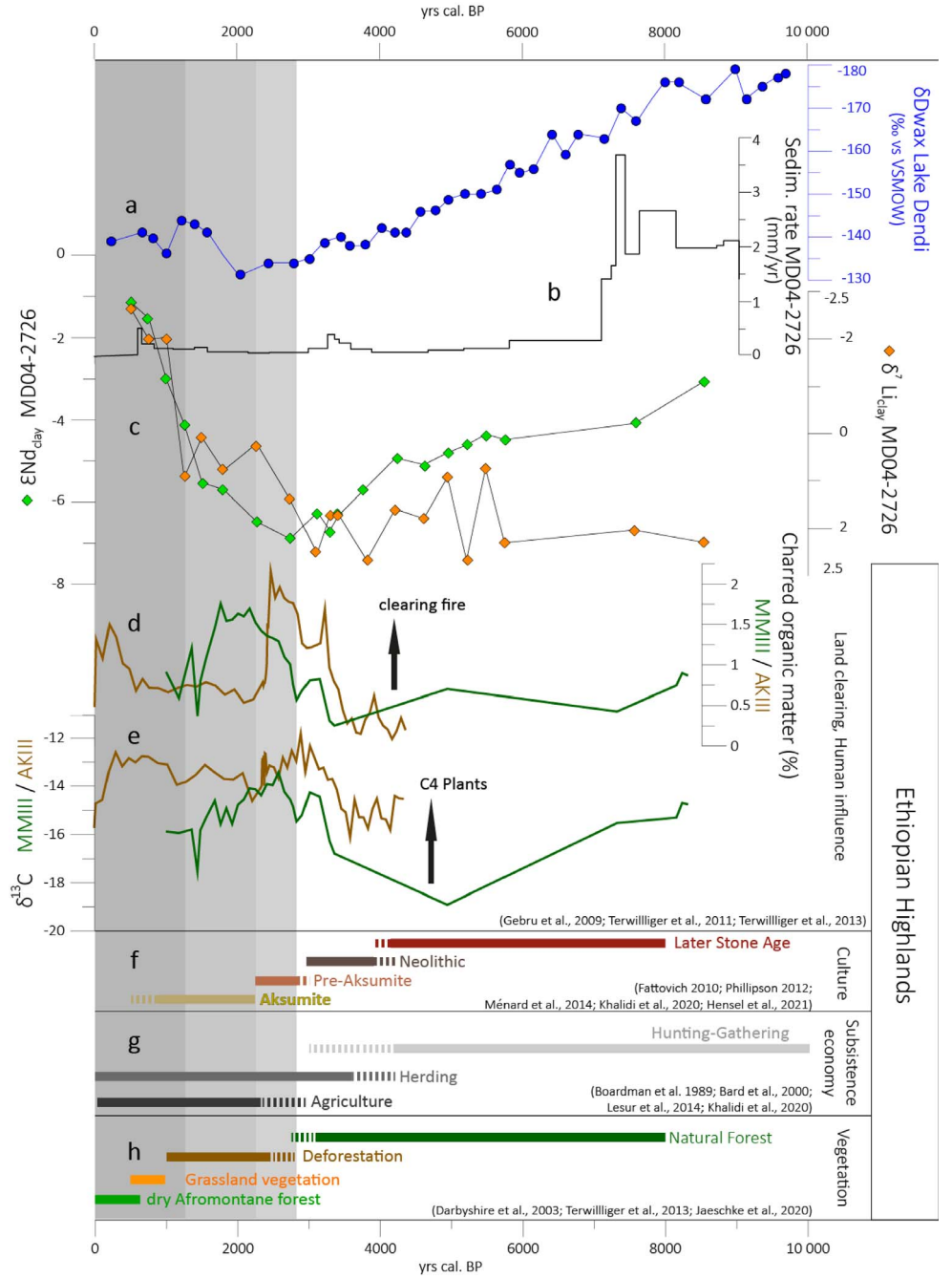

Figure 3. A diagram illustrating paleoenvironmental proxies in association with an archaeological timeline for East Africa during the Holocene. (a) δD_{wax} of Lake Dendi [Jaeschke et al., 2020]; (b) sedimentation rate of core MD04-2726; (c) εNd (light green) and δ^7Li (orange) in clay-size fractions of core MD04-2726; (d) charred organic matter (%) of Mai Maikden (MMIII, green line) and Adi Kolen (AKIII, brown line) soil profiles [Gebru et al., 2009, Terwilliger et al., 2011, 2013]; (e) δ^{13}C of Mai Maikden (MMIII, green line) and Adi Kolen (AKIII, brown line) soil profiles [Gebru et al., 2009, Terwilliger et al., 2011, 2013]. Changes in: (f) Human culture [after Fattovich, 2010, Hensel et al., 2019, Khalidi et al., 2020, Ménard et al., 2014, Phillipson, 2012], (g) Subsistence economy [after Bard et al., 2000, Boardman, 1999, Khalidi et al., 2020, Lesur et al., 2014], (h) Vegetation [after Darbyshire et al., 2003, Terwilliger et al., 2013, Jaeschke et al., 2020] across the Ethiopian highlands.

Table 1. δ^7Li_{clay} and εNd_{clay} data for clays from the MD04-2726 core

ID Clay sample	Depth (cm)	Age (years cal. BP)	δ^7Li (‰)	εNd	2σ
C5	1	501	−2.64	−1.14	0.29
C7	5	751	−2	−1.53	0.25
C14	9	1000	−2.04	−3.03	0.25
C3	13	1248	0.93	−4.11	0.19
C6	17	1497	0.076	−5.53	0.26
C9	21	1801	0.78	−5.7	0.3
C13	25	2269	0.21	−6.48	0.22
C15	29	2737	1.39	−6.89	0.24
C11	33	3115	2.525	−6.25	0.26
C2	37	3290	1.74	−6.69	0.23
C4	41	3409	1.69	−6.33	0.25
C1	45	3810	2.67	−5.63	0.37
C18	49	4212	1.59	−4.93	0.23
C16	53	4613	1.79	−5.09	0.24
C8	57	4948	0.92	−4.8	0.21
C10	61	5215	2.67	−4.61	0.26
C17	65	5482	0.74	−4.35	0.23
C12	69	5750	2.3	−4.48	0.26
C20	128	7564	2.03	−4.09	0.19
C19	186	8543	2.29	−3.06	0.26

in the Ethiopian Highlands [Garzanti et al., 2015]. This can be explained by Blue Nile seasonal discharge, supported by summer monsoon precipitations even during arid periods [Harrower et al., 2020, Sulas, 2014].

Overall, the radiogenic εNd signature of clay-size fractions in cores MD04-2726 and MS27PT indicate a Blue Nile/Ethiopian Traps provenance over the last ~3000 years. A reworking of Ethiopian clay can be excluded because it would result in a shift toward lower, rather than higher εNd values. Previously deposited sediments with high radiogenic εNd values could have been reworked by the intensive irrigation management conducted along the Nile mainstream during the Ptolemaic or Roman periods, concomitant with the development of the Aksumite civilization [Flaux et al., 2012, Pennington et al., 2017, Stanley and Bernhardt, 2010]. However, in that case, one would have expected a shift towards lower εNd values. Indeed, basaltic Nd values (εNd = −2 to ~0) of Ethiopian Traps origin would have been diluted by the input of sediments with the lowest εNd values originating from the White Nile River (εNd = −13.3) and from aeolian sources, which are not preserved [εNd = −15; from the Saharan Metacraton; Abdelsalam et al., 2002, Garzanti et al., 2015].

Altogether, the low δ^7Li and high εNd signatures of the Late Holocene support a strong non-climatic forcing of chemical weathering conditions in the Ethiopian Traps. These results are at odds with what would normally be expected based on the arid hydroclimatic conditions in East Africa during this period and based on chemical weathering trends observed over the last 100 ka. In consequence, we suggest that anthropogenic control was a probable driving force of chemical weathering in the Ethiopian Highlands.

4.1.1. *Concomitant increase of land use and chemical weathering since 3000 BP in the Ethiopian highlands*

East Africa is widely known as one of the cradles of humankind because the volcano-tectonic formation

Table 2. δ^7Li_{clay} and εNd_{clay} data measured in the clay fractions from the MS27PT core

ID Clay sample	Depth (cm)	Age (years cal. BP)	δ^7Li (‰)	2σ	εNd	2σ
A28	2	1258	−1.15	0.01	−5.69	0.1
A24	7	2640	0.47	0.06	−6.97	0.14
A33	11	3449	1.45	0.01	−7	0.2
A30	17	4923	1.72	0.01	−5.01	0.12
A2	22	5925	2.02	0.06	−4.51	0.16
A22	35	7430	1.47	0.02	−3.64	0.13
A46	39	7582	1.85	0.02	−2.45	0.14
A34	52	7946	1.82	0.02	−3.62	0.17
A29	54	8007	1.8	0.01	−3.81	0.12
L21	70	8403	2.11	0.06		
A48	82	8551	2.14	0.01	−2.1	0.13
L22	95	8712	2.47	0.04		
A3	102	8891	2.83	0.02	−4.2	0.19
A39	111	8980	1.95			
A35	114	8999	2.49	0.01	−2.27	0.12
L23	120	9068	1.88	0.08		
A57	137	9203	1.79	0.01	−2.98	0.17
A5	152	9338	2.41	0.02	−3.01	0.23
A47	172	9498	1.72	0.01	−1.73	0.17
A58	194	9683	2.04	0.01	−2.34	0.27
L24	206	9820	2.43	0.06		
L26	243	11,165	1.81	0.05		
L27	255	11,601	1.89	0.06		
A6	263	11,892	2.27	0.02	−0.98	0.17
A31	269	12,074	2.15	0.01	−2.82	0.2
A44	274	12,256	1.73	0.01	−2.65	0.23
A27	278	12,522	1.66	0.02	−1.99	0.12
A25	281	12,695	1.53	0.02	−2.76	0.11
A7	283	12,810	1.79	0.02	−2.11	0.15
A54	289	13,309	1.99	0.02	−1.97	0.2
A56	296	14,588	1.62	0.02	−3.65	0.14
	296	14,934	1.98	0.04	−4.24	0.12
A8	298	15,280	2.58	0.02	−5.44	0.17
A45	300	16,635	2.03	0.02	−5.25	0.16
A9	300	17,989	3.08	0.02	−6.88	0.14
A55	301	18,855	2.59	0.01	−5.63	0.22
A32	303	20,588	2.61	0.02	−5.97	0.15
B6	304	21,024	2.22	0.03	−6.63	0.31
B4	305	21,461	2.52	0.04	−6.01	0.14

(continued on next page)

Table 2. (continued)

ID Clay sample	Depth (cm)	Age (years cal. BP)	δ^7Li (‰)	2σ	εNd	2σ
A10	306	21,897	3.63	0.01	−5.82	0.16
B5	307	22,334	2.88	0.04	−5.99	0.14
B8	308	22,770	4	0.03	−6.4	0.23
A37	310	23,207	2.65	0.01	−5.66	0.18
B9	310	23,643	2.51	0.03	−5.23	0.12
B11	311	24,079	2.87	0.03	−5.25	0.12
B10	312	24,516	3.16	0.04	−4.95	0.08
B12	313	24,952	3.12	0.04	−5.7	0.14
B14	314	25,389	1.77	0.08	−6.18	0.16
A36	316	25,825	0.93	0.01	−4.83	0.18
A60	317	26,411	1.92	0.01	−5.05	0.16
B3	321	27,630	1.65	0.04	−3.9	0.16
B7	323	28,312	1.86	0.04	−4.74	0.27
A61	325	28,994	1.74	0.01	−4.08	0.33
B2	327	29,677	2.09	0.03	−4.68	0.45
B1	329	30,359	2.02	0.02	−3.26	0.12
A59	331	31,041	1.3	0.01	−4.29	0.18
D3	335	31,881	1.53	0.04	−3.64	0.25
D10	343	32,107	2.12	0.04	−3.75	0.22
D12	357	34,078	3.09	0.02	−4.67	0.25
E9	370	37,689	2.48	0.04	−3.55	0.22
E3	374	38,841	2.83	0.03	−4.09	0.21
E19	375	39,024	2.56	0.04	−4.56	0.23
E15	376	39,101	2.82	0.03	−4.15	0.25
E4	377	39,183	3.31	0.02	−4.65	0.23
D8	385	41,627	2.34	0.03	−4.01	0.25
E12	395	46,755	1.52	0.03	−3.6	0.32
E14	397	47,811	1.72	0.02	−4.98	0.22
E2	398	48,339	2	0.03	−4.66	0.22
F6	399	48,630	1.98			
E8	400	49,081	1.81	0.01	−3.62	0.22
F4	403	50,015	2.27			
F3	408	51,572	2.44			
F2	414	53,440	1.95			
E18	419	54,997	4.27	0.06	−2.66	0.24
F5	421	55,619	3.34			
F1	429	58,110	1.98			
D7	440	61,535	0.03	2.7	−3.29	0.24
D9	443	62,469	2.87	0.02	−3.03	0.25

(continued on next page)

Table 2. (continued)

ID Clay sample	Depth (cm)	Age (years cal. BP)	δ^7Li (‰)	2σ	εNd	2σ
D2	447	63,715	2.52	0.04	−5.18	0.26
E1	448	64,026	3.09	0.02	−5.15	0.24
E11	451	64,960	2.08	0.02	−5.09	0.23
D4	455	66,206	2.21	0.03	−6.66	0.23
D11	459	67,275	1.92	0.04	−7.55	0.25
D1	469	72,290	2.17	0.03	−4.99	0.25
D5	476	74,500	2.9	0.03	−4.4	0.27
E7	495	78,500	3.01	0.02	−4.17	0.24
E5	506	79,600	3.38	0.03	−4.41	0.25
D6	520	81,000	3.45	0.03	−4.09	0.24
D20	540	83,000	3.67	0.05	−3.9	0.23
D15	553	84,300	3.52	0.03	−4.1	0.25
E13	567	85,700	3.41	0.02	−3.71	0.23
E17	578	87,320	2.96	0.02	−3.58	0.23
D19	590	89,374	2.71	0.03	−3.59	0.24
D16	597	90,455	3.09	0.03	−5.66	0.23
D13	602	91,201	2.67	0.04	−3.85	0.26
D18	609	92,080	3.99	0.03	−7.69	0.23
D22	617	93,085	2.14	0.04	−6.03	0.26
E16	627	94,341	2.95	0.02	−4.44	0.26
D17	641	96,100	3.03	0.03	−4.65	0.26
E22	645	96,603	3.07	0.02	−4.27	0.2
E6	666	99,304	3.28	0.02	−3.71	0.22
D14	679	100,874	2.99	0.01	−3.8	0.24
E10	694	102,758	3.45	0.02	−3.47	0.25
D23	705	104,140	2.99	0.02	−3.97	0.2
D25	712	105,020	2.76	0.02	−4.42	0.25
D24	719	105,899	3.15	0.03	−3.74	0.23

of the East African Rift System created the ideal living conditions for early hominins and for the preservation of their remains [WoldeGabriel et al., 2001]. Comprehensive archaeological studies have demonstrated that during the long period of transition from solely hunter-gathering, to herding around 12 to 3 ka cal. BP, populations were relatively well adapted to the effects of hydrological changes in the region as a result of flexible mobility and subsistence strategies [Chritz et al., 2019, Khalidi et al., 2020, Kuper and Kröpelin, 2006, Mologni et al., 2021, Wright et al., 2015]. The Late Holocene witnessed a gradual aridification during which the first East African complex polities in Highland Ethiopia and Eritrea developed and integrated agriculture into their socio-economic fabric [Boardman, 1999]. The Ethiopian plateau, located in the headwaters region of the Blue Nile, saw the emergence of the first Pre-Aksumite polities around 3000 BP, followed by the foundation of the first Aksumite urban settlements around ~2000 years cal. BP [Fattovich, 2010, Phillipson, 2012]. Extending over the source region of the Blue Nile and Atbara/Tezeke rivers, the pre-Axumite to Axumite period was accompanied by the intensification of agricultural practices [Blond et al., 2018; Figure 1b; Boardman, 1999]. Even if the use of irrigation systems

was not necessary because of abundant seasonal monsoonal rainfall [Harrower et al., 2020], anthropic small-scale management of primary landscapes became widespread across the highland region [Blond et al., 2018, Sulas, 2014]. From ~2600 BP onwards, increasing demographic pressure over the Ethiopian highlands was accompanied by intensified land use and deforestation [Darbyshire et al., 2003], soil degradation [Bard et al., 2000] and water management [Blond et al., 2018, Federica and Innocent, 2018, Sulas, 2014, Sulas et al., 2009]. Organic proxy investigations of soil profiles from the headwaters region of the Atbara/Tekeze rivers (Adi Kolan=AKIII, Mai Maikden=MMIII; Figure 1b) revealed a strong increase in land clearing and anthropogenic fire activity between ~3000 and ~2000 years cal. BP [Gebru et al., 2009, Terwilliger et al., 2013, 2011; Figure 3c, d]. Other proxies such as hydrogen (HI) and oxygen (OI) indices from Rock-Eval pyrolysis also indicated intense chemical alteration of organic matter due to agricultural humidification processes and/or human-induced fires [Terwilliger et al., 2013, 2011]. Such extensive anthropogenic landscape management had a major impact on the pedogenic system, leading to an increase of soil leaching, and potentially explaining the decrease of δ^7Li values during this period.

In this context, the δ^7Li proxy evidence for enhanced chemical weathering in the Ethiopian Traps starting ~3000 BP is concomitant with anthropogenic landscape degradation recorded during the Pre-Aksumite and Aksumite periods (Figure 3). During the same period, large erosion rates in the Ethiopian highlands were recorded in Lake Dendi sediment records, in agreement with intensive land-use activity [Jaeschke et al., 2020].

Overall, the concomitance between the intensification of land use beginning around 3000 BP and enhanced soil alteration (inferred from negative δ^7Li values) suggests that agricultural management systems played a key role in this dramatic shift. The impact of human activities on Li isotopes appears clearly distinct from the effect induced by an increase in precipitation during high insolation periods. It should be specified that the area of the Pre-Aksumite and Aksumite polities to which our results refer are those drained by tributaries of the Nile River, which cover only one part of the overall territory of these polities (Figure 1b). Consequently, our results reflect the impact of anthropic activities in regions that were part of the territory of the Aksumite kingdom and its precursors, and not necessarily that of the main centres [Fattovich, 2010, Phillipson, 2012].

It is interesting to note that paleolimnological and historical data obtained for the Late Holocene record of Lake Fayum along the northern Nile indicate an increase of land-use since ~4 ka BP, hence 1000 years earlier than the observed εNd shift in our NDSF cores [Butzer, 1997, Hamdan et al., 2020, Hassan et al., 2006]. Similarly, various indices of land-use intensification in the Nile delta have been recorded since ~4 ka BP [Zhang et al., 2022a,b]. The fact that there was a recorded increase of human activities in the Nile delta and no change in εNd signature around 4 Ka BP indicates that the reworking of fine-grained sediments with radiogenic Nd isotopic signatures and erosion processes were negligible during this period. In contrast, the co-evolution of chemical weathering (inferred from δ^7Li) and intensive land-use patterns associated with pre-Aksumite and Aksumite complex polities (inferred from εNd and sedimentological evidence) over the last 3000 years suggest that the increase of chemical weathering intensity was mostly generated in the Blue Nile basin, and therefore in the basaltic highlands. Further high resolution studies of local pedo-sedimentary archives will be needed in order to more precisely quantify the effects of land use on weathering in this region, and which may be more significant than what has been illustrated by studies of deltaic sediments.

4.2. *Towards a global scale impact of anthropogenic activities on Earth systems since the late Holocene?*

As discussed above, the combined Nd and Li isotope records are consistent with an increase of chemical weathering intensity in the Ethiopian highlands (Figure 4a). This is during a period characterized by deforestation, the development of agriculture, water management, and the exploitation of soil resources attributed to pre-Aksumite and Aksumite polities between 3000 and 1000 years cal. BP. This finding is consistent with the hypothesis of an early anthropogenic forcing in the Nile River Basin, adding further evidence to the large scale impact of prehistoric human activities on continental weathering.

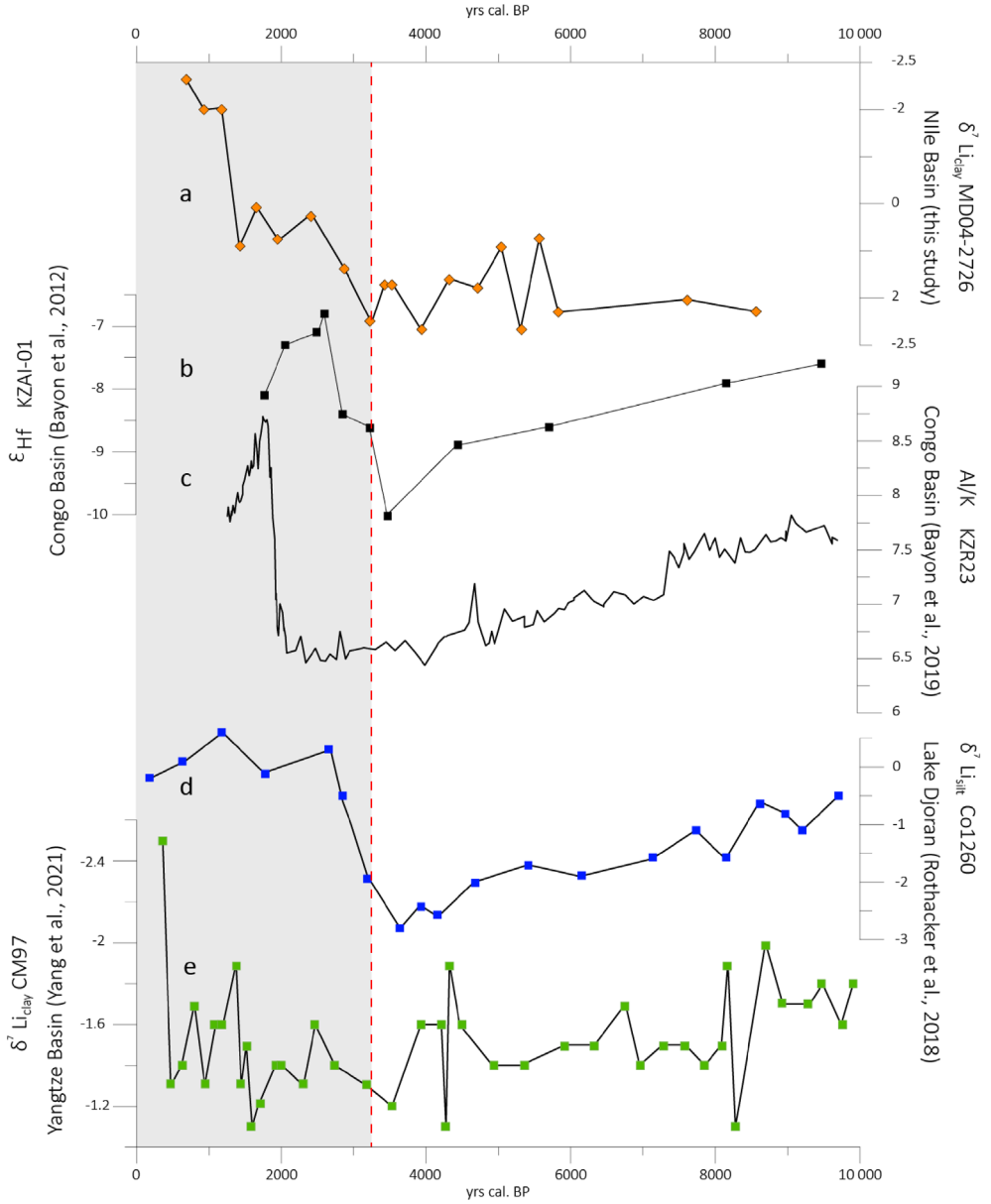

Figure 4. Diagram illustrating the intensity of continental chemical weathering worldwide during the Late Holocene. (a) clay δ^7Li of MD04-2726 core (this study); (b) εHf variations in KZAl-01 core [Congo basin; Bayon et al., 2012]; (c) Bulk sediment Al/K ratio in KZR23 core [Congo basin; Bayon et al., 2019]; (d) silt δ^7Li of Co1260 [Djoran Lake; Rothacker et al., 2018]; (e) Clay δ^7Li evolution determined for the CM97 core [Yangtze basin; Yang et al., 2021].

Several compelling comparisons can be made with other large continental regions. In highland Yemen, a direct correlation has been made between combined settlement increase, development of terraced agriculture, environmental degradation and soil erosion during the Yemen Bronze Age [between 5000 and 4000 BP; Wilkinson, 2005, 1997]. Similarly to Ethiopia, Yemen highland erosion is attributed to

the combination of climatic drying and major societal changes, which left a heavy human footprint on the landscape [Bard et al., 2000, Wilkinson, 1997]. In the Congo Basin, Bayon et al. [2012, 2019] reported an abrupt event of intense chemical weathering during the third millennium BP. During this time interval, the highest aluminum/potassium (Al/K) and hafnium isotopic (εHf; Figure 4b) ratios of the last 40 thousand years were encountered in deltaic records recovered near the mouth of the Congo River. In Central Africa, this weathering event coincided with a collapse of the rainforest and accelerated soil erosion, but also with the southward migration of Bantu-speaking people from a region located between Nigeria and Cameroon [Bayon et al., 2019, 2012, Garcin et al., 2018, Saulieu et al., 2021, Seidensticker et al., 2021]. While debate exists about the cause of this major environmental crisis, several authors have suggested that both the vegetation shift and the chemical weathering event were partly caused by an intensification of iron smelting and land use related to the Bantu expansion [Bayon et al., 2012, Garcin et al., 2018, Bayon et al., 2019]. In south-eastern Europe, Rothacker et al. [2018] reported an anomalous (i.e. unrelated to the climate trend) increase of δ^{234}U and δ^{7}Li values in a sedimentary record from Lake Dojran (Greece) over the last 3300 years cal. BP. These isotopic variations have been interpreted as a marker of both intensive soil erosion and chemical weathering (Figure 4c). Combined with additional biomarker data and inferences from archaeological studies, this feature coincided with the first signs of agriculture in the Dojran basin, as well as the development of cultivated and ruderal plants. Eventually, in China, Yang et al. [2021] suggested that small but significant Li isotope fluctuations recorded in a sediment core from the Yangtze delta since ~2 ka, were associated with increase in sedimentation rates, and might be related to the rapid development of agricultural practices and other human activities in the lowland region of the Yangzte River basin (Figure 4d).

Although the number of case studies using chemical weathering proxies remains limited to date, most of them highlight an early anthropogenic forcing on continental chemical weathering over the last few thousand years. Additional high temporal resolution studies are now needed in order to determine the late Holocene origin and evolution of chemical weathering at a global scale, and to precisely quantify the environmental impact caused by the rise of early polities worldwide.

5. Conclusions

Over recent years, arguments in favour of human-induced climate alteration during prehistoric times have provided support for the Early Anthropogenic Hypothesis. However, the impact of human activities on chemical weathering and on Earth surface processes remains poorly documented. In this article, we have explored the relationships between the evolution of soil weathering and the rise of early complex polities and urban societies in East Africa, namely during the Pre-Aksumite and Aksumite periods. Using Nd (εNd) and Li (δ^{7}Li) isotopes in the clay-size fraction of marine sediments retrieved from the Nile Deep Sea Fan, we reconstructed the evolution of continental weathering in the Nile Basin over the last 9 ka. Our results show a trend towards higher εNd and very low δ^{7}Li values over the last 3000 years cal. BP, indicating both enhanced weathering processes and sediment transport from the area of the Ethiopian highlands drained by the Blue Nile. The negative δ^{7}Li values, which are unprecedented over the last 100 ka, suggest that this event cannot be explained by natural hydroclimatic forcing. Instead, using archaeological, paleo-pedological and paleo-botanical data, we observed that this weathering event was concomitant with the emergence and rise of the Pre-Aksumite and Aksumite polities, which developed after 3000 ka BP in the headwaters region of the Blue Nile. The association between the onset of intensive agricultural and hydrological management by Pre-Axumite and Aksumite populations, and enhanced chemical weathering in the Blue Nile catchment points towards an early anthropogenic degradation of soils in East Africa. Taken together with other case-studies and proxy records worldwide, we posit that human activities have acted as a major driver of continental chemical weathering since 4.3-3 ka BP, driving the hypothesis of an Earlier Anthropogenic disruption of the Earth Critical Zone over a larger scale.

Conflicts of interest

Authors have no conflict of interest to declare.

Acknowledgements

This work was financially supported by BQR Geoazur- OCA, an INSU-SYSTER grant and the ANR INTOCC (ANR-15-CE31-0013). The MS27PT and MD04-2726 cores were recovered during the MIMES and VANIL cruises respectively. We greatly thank Philipe Télouk for his help with the MC-ICP-MS at the CNRS-INSU national service at Lyon.

References

Abdelsalam, M. G., Liégeois, J.-P., and Stern, R. J. (2002). The saharan metacraton. *J. Afr. Earth Sci.*, 34, 119–136.

Anfray, F. (1967). Maṭarā. *Ann. d'Éthiopie*, 7, 33–88.

Balter, V. and Vigier, N. (2014). Natural variations of lithium isotopes in a mammalian model. *Metallomics*, 6, 582–586.

Bard, K. A., Coltorti, M., DiBlasi, M. C., Dramis, F., and Fattovich, R. (2000). The environmental history of tigray (Northern Ethiopia) in the middle and late holocene: a preliminary outline. *Afr. Archaeol. Rev.*, 17, 65–86.

Bastian, L., Revel, M., Bayon, G., Dufour, A., and Vigier, N. (2017). Abrupt response of chemical weathering to late quaternary hydroclimate changes in northeast Africa. *Sci. Rep.*, 7, article no. 44231.

Bastian, L., Vigier, N., Revel, M., Yirgu, G., Ayalew, D., and Pik, R. (2019). Chemical erosion rates in the upper Blue Nile Basin and related atmospheric CO_2 consumption. *Chem. Geol.*, 518, 19–31.

Bastian, L. & Mologni, C., Vigier, N., Bayon, G., Lamb, H., Bosch, D., Kerros, M.-E., Colin, C., and Revel, M. (2021). Co-variations of climate and silicate weathering in the Nile Basin during the Late Pleistocene. *Quat. Sci. Rev.*, 264, article no. 107012.

Bayon, G., Dennielou, B., Etoubleau, J., Ponzevera, E., Toucanne, S., and Bermell, S. (2012). Intensifying weathering and land use in iron age Central Africa. *Science*, 335, 1219–1222.

Bayon, G., Schefuss, E., Dupont, L., Borges, A. V., Dennielou, B., Lambert, T., Mollenhauer, G., Monin, L., Ponzevera, E., Skonieczny, C., and Andre, L. (2019). The roles of climate and human land-use in the late Holocene rainforest crisis of Central Africa. *Earth Planet. Sci. Lett.*, 505, 30–41.

Bayon, G., Toucanne, S., Skonieczny, C., André, L., Bermell, S., Cheron, S., Dennielou, B., Etoubleau, J., Freslon, N., Gauchery, T., Germain, Y., Jorry, S. J., Ménot, G., Monin, L., Ponzevera, E., Rouget, M.-L., Tachikawa, K., and Barrat, J. A. (2015). Rare earth elements and neodymium isotopes in world river sediments revisited. *Geochim. Cosmochim. Acta*, 170, 17–38.

Berger, A. and Loutre, M. F. (1991). Insolation values for the climate of the last 10 million years. *Quat. Sci. Rev.*, 10, 297–317.

Blanchet, C. L. (2019). A global database of radiogenic Nd and Sr isotopes in marine and terrestrial samples (V.2.0). https://doi.org/10.5880/GFZ.4.3.2019.001. GFZ Data Services, Potsdam.

Blanchet, C. L., Contoux, C., and Leduc, G. (2015). Runoff and precipitation dynamics in the blue and white nile catchments during the mid-Holocene: A data-model comparison. *Quat. Sci. Rev.*, 130, 222–230.

Blanchet, C. L., Frank, M., and Schouten, S. (2014). Asynchronous changes in vegetation, runoff and erosion in the nile river watershed during the holocene. *PLoS One*, 9, article no. e115958.

Blanchet, C. L., Osborne, A. H., Tjallingii, R., Ehrmann, W., Friedrich, T., Timmermann, A., Brückmann, W., and Frank, M. (2021). Drivers of river reactivation in North Africa during the last glacial cycle. *Nat. Geosci.*, 14, 97–103.

Blanchet, C. L., Tjallingii, R., Frank, M., Lorenzen, J., Reitz, A., Brown, K., Feseker, T., and Brückmann, W. (2013). High- and low-latitude forcing of the Nile River regime during the Holocene inferred from laminated sediments of the Nile deep-sea fan. *Earth Planet. Sci. Lett.*, 364, 98–110.

Blond, N., Jacob-Rousseau, N., and Callot, Y. (2018). Terrasses alluviales et terrasses agricoles. Première approche des comblements sédimentaires et de leurs aménagements agricoles depuis 5000 av. n. è. à Wakarida (Éthiopie). *Geomorphologie*, 24, 277–300.

Boardman, S. (1999). The Agricultural Foundation of the Aksumite Empire, Ethiopia. In van der Veen, M., editor, *The Exploitation of Plant Resources in Ancient Africa*, pages 137–147. Springer US, Boston, MA.

Bouchez, J., Blanckenburg, F., and von Schuessler, J. A. (2013). Modeling novel stable isotope ratios in the weathering zone. *Am. J. Sci.*, 313, 267–308.

Butzer, K. W. (1997). Late quaternary problems of the

Egyptian Nile: stratigraphy, environments, prehistory. *Paleo*, 23, 151–173.

Carignan, J., Vigier, N., and Millot, R. (2007). Three secondary reference materials for Lithium Isotope Measurements: Li7-N, Li6-N and LiCl-N Solutions. *Geostand. Geoanal. Res.*, 31, 7–12.

Caves Rugenstein, J. K., Ibarra, D. E., and von Blanckenburg, F. (2019). Neogene cooling driven by land surface reactivity rather than increased weathering fluxes. *Nature*, 571, 99–102.

Chritz, K. L., Cerling, T. E., Freeman, K. H., Hildebrand, E. A., Janzen, A., and Prendergast, M. E. (2019). Climate, ecology, and the spread of herding in eastern Africa. *Quat. Sci. Rev.*, 204, 119–132.

Costa, K., Russell, J., Konecky, B., and Lamb, H. (2014). Isotopic reconstruction of the African humid period and congo air boundary migration at Lake Tana, Ethiopia. *Quat. Sci. Rev.*, 83, 58–67.

Darbyshire, I., Lamb, H., and Umer, M. (2003). Forest clearance and regrowth in northern Ethiopia during the last 3000 years. *The Holocene*, 13, 537–546.

Dellinger, M., Bouchez, J., Gaillardet, J., Faure, L., and Moureau, J. (2017). Tracing weathering regimes using the lithium isotope composition of detrital sediments. *Geology*, 45, 411–414.

Dosseto, A., Vigier, N., Joannes-Boyau, R., Moffat, I., Singh, T., and Srivastava, P. (2015). Rapid response of silicate weathering rates to climate change in the Himalaya. *Geochem. Perspect. Lett.*, 1, 10–19.

Fattovich, R. (2010). The development of ancient states in the Northern Horn of Africa, c. 3000 BC–AD 1000: An archaeological outline. *J. World Prehist.*, 23, 145–175.

Federica, S. and Innocent, P. (2018). *Water and Society from Ancient Times to the Present: Resilience, Decline and Revival*. Routledge/Taylor & Francis Group, London; New York, 1st edition.

Flaux, C., El-Assal, M., Marriner, N., Morhange, C., Rouchy, J.-M., Soulié-Märsche, I., and Torab, M. (2012). Environmental changes in the Maryut lagoon (northwestern Nile delta) during the last ~2000 years. *J. Archaeol. Sci.*, 39, 3493–3504.

Garcin, Y., Deschamps, P., Ménot, G., de Saulieu, G., Schefuß, E., Sebag, D., Dupont, L. M., Oslisly, R., Brademann, B., Mbusnum, K. G., Onana, J.-M., Ako, A. A., Epp, L. S., Tjallingii, R., Strecker, M. R., Brauer, A., and Sachse, D. (2018). Early anthropogenic impact on Western Central African rainforests 2,600 y ago. *Proc. Natl. Acad. Sci. USA*, 115, 3261–3266.

Garzanti, E., Andò, S., Padoan, M., Vezzoli, G., and El Kammar, A. (2015). The modern Nile sediment system: Processes and products. *Quat. Sci. Rev.*, 130, 9–56.

Gebru, T., Eshetu, Z., Huang, Y., Woldemariam, T., Strong, N., Umer, M., DiBlasi, M., and Terwilliger, V. J. (2009). Holocene palaeovegetation of the Tigray Plateau in northern Ethiopia from charcoal and stable organic carbon isotopic analyses of gully sediments. *Palaeogeogr. Palaeoclimatol. Palaeoecol.*, 282, 67–80.

Gerlach, I., editor (2015). *South Arabia and its Neighbours: Phenomena of Intercultural Contacts. Proceedings of the 14th Rencontres Sabéennes*, volume 14 of *Archäologische Berichte aus dem Yemen*. Reichert, Wiesbaden.

Grousset, F., Biscaye, P. E., Zindler, A., Prospero, J., and Chester, R. (1988). Neodymium isotopes as tracers in marine sediments and aerosols: North Atlantic. *Earth Planet. Sci. Lett.*, 87, 367–378.

Grousset, F. E. and Biscaye, P. E. (2005). Tracing dust sources and transport patterns using Sr, Nd and Pb isotopes. *Chem. Geol.*, 222, 149–167.

Hamdan, M. A., Flower, R. J., Hassan, F. A., and Hassan, S. M. (2020). The Holocene history of the Faiyum Lake (Egypt) based on sediment characteristics, diatoms and ostracods contents. *J. Great Lakes Res.*, 46, 456–475.

Harrower, M. J., Nathan, S., Mazzariello, J. C., Zerue, K., Dumitru, I. A., Meresa, Y., Bongers, J. L., Gebreegziabher, G., Zaitchik, B. F., and Anderson, M. C. (2020). Water, geography, and aksumite civilization: the southern red sea archaeological histories (SRSAH) project survey (2009–2016). *Afr. Archaeol. Rev.*, 37, 51–67.

Hassan, F. A., Tassie, G., Flower, R., Hughes, R., and Hamdan, M. A. (2006). Modeling environmental and settlement change in the Faiyum. *Egypt. Archaeol.*, 29, 37–40.

Hensel, E. A., Bödeker, O., Bubenzer, O., and Vogelsang, R. (2019). Combining geomorphological–hydrological analyses and the location of settlement and raw material sites—a case study on understanding prehistoric human settlement activity in the southwestern Ethiopian Highlands. *E&G Quat. Sci. J.*, 68, 201–213.

Hindshaw, R. S., Tosca, N. J., Piotrowski, A. M., and Tipper, E. T. (2018). Clay mineralogy, strontium and neodymium isotope ratios in the sediments of two High Arctic catchments (Svalbard). *Earth Surf. Dyn.*, 6, 141–161.

Jacobsen, S. B. and Wasserburg, G. J. (1980). Sm–Nd isotopic evolution of chondrites. *Earth Planet. Sci. Lett.*, 50, 139–155.

Jaeschke, A., Thienemann, M., Schefuß, E., Urban, J., Schäbitz, F., Wagner, B., and Rethemeyer, J. (2020). Holocene hydroclimate variability and vegetation response in the ethiopian highlands (Lake Dendi). *Front. Earth Sci.*, 8, article no. 585770.

Japp, S. (2019). Yeha, Äthiopien. Archäologische Untersuchungen auf dem Kirchenvorplatz von Yeha. Die Arbeiten der Jahre 2013 bis 2018. *e-Forschungsberichte*, 1, 14–18.

Khalidi, L., Mologni, C., Ménard, C., Coudert, L., Gabriele, M., Davtian, G., Cauliez, J., Lesur, J., Bruxelles, L., Chesnaux, L., Redae, B. E., Hainsworth, E., Doubre, C., Revel, M., Schuster, M., and Zazzo, A. (2020). 9000 years of human lakeside adaptation in the Ethiopian Afar: Fisher-foragers and the first pastoralists in the Lake Abhe basin during the African humid period. *Quat. Sci. Rev.*, 243, article no. 106459.

Krissansen-Totton, J. and Catling, D. C. (2017). Constraining climate sensitivity and continental versus seafloor weathering using an inverse geological carbon cycle model. *Nat. Commun.*, 8, article no. 15423.

Kuper, R. and Kröpelin, S. (2006). Climate-controlled Holocene occupation in the Sahara: motor of Africa's evolution. *Science*, 313, 803–807.

Kutzbach, J. E., Guan, J., He, F., Cohen, A. S., Orland, I. J., and Chen, G. (2020). African climate response to orbital and glacial forcing in 140,000-y simulation with implications for early modern human environments. *Proc. Natl. Acad. Sci. USA*, 117, 2255–2264.

Lesur, J., Hildebrand, E. A., Abawa, G., and Gutherz, X. (2014). The advent of herding in the Horn of Africa: New data from Ethiopia, Djibouti and Somaliland. *Quat. Int.*, 343, 148–158.

Lin, H. S. (2009). Earth's critical zone and hydropedology. *Hydrol. Earth Syst. Sci.*, 6, 3417–3481.

Manning, J. G., Ludlow, F., Stine, A. R., Boos, W. R., Sigl, M., and Marlon, J. R. (2017). Volcanic suppression of Nile summer flooding triggers revolt and constrains interstate conflict in ancient Egypt. *Nat. Commun.*, 8, article no. 900.

McGee, D. and deMenocal, P. B. (2017). Climatic changes and cultural responses during the african humid period recorded in multi-proxy data. In *Oxford Research Encyclopedia of Climate Science*. Oxford University Press, Oxford.

Ménard, C., Bon, F., Dessie, A., Bruxelles, L., Douze, K., Fauvelle, F.-X., Khalidi, L., Lesur, J., and Mensan, R. (2014). Late stone age variability in the main Ethiopian rift: new data from the Bulbula River, Ziway–Shala basin. *Quat. Int.*, 343, 53–68.

Ménot, G., Pivot, S., Bouloubassi, I., Davtian, N., Hennekam, R., Bosch, D., Ducassou, E., Bard, E., Migeon, S., and Revel, M. (2020). Timing and stepwise transitions of the African humid period from geochemical proxies in the nile deep-sea fan sediments. *Quat. Sci. Rev.*, 228, article no. 106071.

Michalopoulos, P. and Aller, R. C. (2004). Early diagenesis of biogenic silica in the Amazon delta: alteration, authigenic clay formation, and storage. *Geochim. Cosmochim. Acta*, 68, 1061–1085.

Misra, S. and Froelich, P. N. (2012). Lithium isotope history of cenozoic seawater: changes in silicate weathering and reverse weathering. *Science*, 335, 818–823.

Mologni, C., Bruxelles, L., Schuster, M., Davtian, G., Ménard, C., Orange, F., Doubre, C., Cauliez, J., Taezaz, H. B., Revel, M., and Khalidi, L. (2021). Holocene East African monsoonal variations recorded in wave-dominated clastic paleoshorelines of Lake Abhe, Central Afar region (Ethiopia & Djibouti). *Geomorphology*, 391, article no. 107896.

Mologni, C., Revel, M., Blanchet, C., Bosch, D., Develle, A.-L., Orange, F., Bastian, L., Khalidi, L., Ducassou, E., and Migeon, S. (2020). Frequency of exceptional Nile flood events as an indicator of Holocene hydro-climatic changes in the Ethiopian highlands. *Quat. Sci. Rev.*, 247, article no. 106543.

Pausata, F. S. R., Gaetani, M., Messori, G., Berg, A., Maia de Souza, D., Sage, R. F., and deMenocal, P. B. (2020). The greening of the Sahara: past changes and future implications. *One Earth*, 2, 235–250.

Pennington, B. T., Sturt, F., Wilson, P., Rowland, J., and Brown, A. G. (2017). The fluvial evolution of the Holocene Nile Delta. *Quat. Sci. Rev.*, 170, 212–231.

Phillipson, D. W. (2012). *Foundations of an African civilization: Aksum & the northern Horn, 1000 BC*

- *AD 1300*. Eastern Africa Series. James Currey, Woodbridge, Suffolk; Rochester, NY.

Pogge von Strandmann, P. A. E., Vaks, A., Bar-Matthews, M., Ayalon, A., Jacob, E., and Henderson, G. M. (2017). Lithium isotopes in speleothems: Temperature-controlled variation in silicate weathering during glacial cycles. *Earth Planet. Sci. Lett.*, 469, 64–74.

Pogge von Strandmann, P. A. E. P., von Kasemann, S. A., and Wimpenny, J. B. (2020). Lithium and lithium isotopes in earth's surface cycles. *Elements*, 16, 253–258.

Revel, M., Colin, C., Bernasconi, S., Combourieu-Nebout, N., Ducassou, E., Grousset, F. E., Rolland, Y., Migeon, S., Bosch, D., Brunet, P., Zhao, Y., and Mascle, J. (2014). 21,000 Years of Ethiopian African monsoon variability recorded in sediments of the western Nile deep-sea fan. *Reg. Environ. Change*, 14, 1685–1696.

Revel, M., Ducassou, E., Grousset, F. E., Bernasconi, S. M., Migeon, S., Revillon, S., Mascle, J., Murat, A., Zaragosi, S., and Bosch, D. (2010). 100,000 Years of African monsoon variability recorded in sediments of the Nile margin. *Quat. Sci. Rev.*, 29, 1342–1362.

Revel, M., Ducassou, E., Skonieczny, C., Colin, C., Bastian, L., Bosch, D., Migeon, S., and Mascle, J. (2015). 20,000 years of Nile River dynamics and environmental changes in the Nile catchment area as inferred from Nile upper continental slope sediments. *Quat. Sci. Rev.*, 130, 200–221.

Rothacker, L., Dosseto, A., Francke, A., Chivas, A. R., Vigier, N., Kotarba-Morley, A. M., and Menozzi, D. (2018). Impact of climate change and human activity on soil landscapes over the past 12,300 years. *Sci. Rep.*, 8, article no. 247.

Ruddiman, W. F. (2003). The anthropogenic greenhouse era began thousands of years ago. *Clim. Chang.*, 61, 261–293.

Ruddiman, W. F., He, F., Vavrus, S. J., and Kutzbach, J. E. (2020). The early anthropogenic hypothesis: A review. *Quat. Sci. Rev.*, 240, article no. 106386.

Saulieu, G., de Garcin, Y., Sebag, D., Nlend, P. R. N., Zeitlyn, D., Deschamps, P., Ménot, G., Carlo, P. D., and Oslisly, R. (2021). Archaeological Evidence for Population Rise and Collapse between ~2500 and ~500 cal. yr BP in Western Central Africa. *Afrique : Archéologie & Arts*, 17, 11–32.

Scheuvens, D., Schütz, L., Kandler, K., Ebert, M., and Weinbruch, S. (2013). Bulk composition of northern African dust and its source sediments—A compilation. *Earth-Sci. Rev.*, 116, 170–194.

Seidensticker, D., Hubau, W., Verschuren, D., Fortes-Lima, C., de Maret, P., Schlebusch, C. M., and Bostoen, K. (2021). Population collapse in Congo rainforest from 400 CE urges reassessment of the Bantu expansion. *Sci. Adv.*, 7, article no. eabd8352.

Sheisha, H., Kaniewski, D., Marriner, N., Djamali, M., Younes, G., Chen, Z., El-Qady, G., Saleem, A., Véron, A., and Morhange, C. (2022). Nile waterscapes facilitated the construction of the Giza pyramids during the 3rd millennium BCE. *Proc. Natl. Acad. Sci. USA*, 119, article no. e2202530119.

Stanley, J.-D. and Bernhardt, C. E. (2010). Alexandria's eastern harbor, Egypt: Pollen, microscopic charcoal, and the transition from natural to human-modified basin. *J. Coast. Res.*, 261, 67–79.

Sulas, F. (2014). Aksum: Water and Urbanization in Northern Ethiopia. In Tvedt, T. and Oestigaard, T., editors, *A History of Water: From Jericho to Cities in the Seas: A History of Urbanization and Water Systems, A History of Water*. I.B.Tauris & Co. Ltd, London.

Sulas, F., Madella, M., and French, C. (2009). State formation and water resources management in the Horn of Africa: the Aksumite Kingdom of the northern Ethiopian highlands. *World Archaeol.*, 41, 2–15.

Tanaka, T., Togashi, S., Kamioka, H., Amakawa, H., Kagami, H., Hamamoto, T., Yuhara, M., Orihashi, Y., Yoneda, S., Shimizu, H., Kunimaru, T., Takahashi, K., Yanagi, T., Nakano, T., Fujimaki, H., Shinjo, R., Asahara, Y., Tanimizu, M., and Dragusanu, C. (2000). JNdi-1: a neodymium isotopic reference in consistency with LaJolla neodymium. *Chem. Geol.*, 168, 279–281.

Terwilliger, V. J., Eshetu, Z., Disnar, J.-R., Jacob, J., Paul Adderley, W., Huang, Y., Alexandre, M., and Fogel, M. L. (2013). Environmental changes and the rise and fall of civilizations in the northern Horn of Africa: An approach combining δD analyses of land-plant derived fatty acids with multiple proxies in soil. *Geochim. Cosmochim. Acta*, 111, 140–161.

Terwilliger, V. J., Zewdu, E., Huang, Y., Alexandre, M., Umer, M., and Tsige, G. (2011). Local variation in climate and land use during the time of the major kingdoms of the Tigray Plateau in Ethiopia and Eritrea. *CATENA*, 85, 130–143.

Thibon, F., Weppe, L., Montanes, M., Telouk, P., and

Vigier, N. (2021). Lithium isotopic composition of reference materials of biological origin TORT-2, DORM-2, TORT-3, DORM-4, SRM-1400 and ERM-CE278k. *J. Anal. At. Spectrom.*, 36, 1381–1388.

Verney-Carron, A., Vigier, N., Millot, R., and Hardarson, B. S. (2015). Lithium isotopes in hydrothermally altered basalts from Hengill (SW Iceland). *Earth Planet. Sci. Lett.*, 411, 62–71.

Vigier, N., Decarreau, A., Millot, R., Carignan, J., Petit, S., and France-Lanord, C. (2008). Quantifying Li isotope fractionation during smectite formation and implications for the Li cycle. *Geochim. Cosmochim. Acta*, 72, 780–792.

Vigier, N., Gislason, S. R., Burton, K. W., Millot, R., and Mokadem, F. (2009). The relationship between riverine lithium isotope composition and silicate weathering rates in Iceland. *Earth Planet. Sci. Lett.*, 287, 434–441.

Wei, G.-Y., Wei, W., Wang, D., Li, T., Yang, X., Shields, G. A., Zhang, F., Li, G., Chen, T., Yang, T., and Ling, H.-F. (2020). Enhanced chemical weathering triggered an expansion of euxinic seawater in the aftermath of the Sturtian glaciation. *Earth Planet. Sci. Lett.*, 539, article no. 116244.

Weldeab, S., Menke, V., and Schmiedl, G. (2014). The pace of East African monsoon evolution during the Holocene: Weldeab et al.; East African monsoon evolution. *Geophys. Res. Lett.*, 41, 1724–1732.

Wilkinson, T. J. (1997). Holocene environments of the high plateau, Yemen. Recent geoarchaeological investigations. *Geoarchaeology*, 12, 833–864.

Wilkinson, T. J. (2005). Soil erosion and valley fills in the Yemen highlands and southern Turkey: Integrating settlement, geoarchaeology, and climate change. *Geoarchaeology*, 20, 169–192.

WoldeGabriel, G., Haile-Selassie, Y., Renne, P. R., Hart, W. K., Ambrose, S. H., Asfaw, B., Heiken, G., and White, T. (2001). Geology and palaeontology of the Late Miocene Middle Awash valley, Afar rift, Ethiopia. *Nature*, 412, 175–178.

Wright, D. K., Forman, S. L., Kiura, P., Bloszies, C., and Beyin, A. (2015). Lakeside view: sociocultural responses to changing water levels of lake Turkana, Kenya. *Afr. Archaeol. Rev.*, 32, 335–367.

Yang, C., Vigier, N., Yang, S., Revel, M., and Bi, L. (2021). Clay Li and Nd isotopes response to hydroclimate changes in the Changjiang (Yangtze) basin over the past 14,000 years. *Earth Planet. Sci. Lett.*, 561, article no. 116793.

Zhang, F., Hu, J., Li, X., Wang, Y., Salem, A., Sun, C., Zhao, X., Zhao, X., Jiang, F., Liu, Y., Shetaia, S. A., and Chen, Z. (2022a). Reconstruction of the Holocene hydro-ecological and environmental change of the Nile Delta: Insights from organic geochemical records in MZ-1 sediment core. *Mar. Geol.*, 443, article no. 106684.

Zhang, X. Y., Gaillardet, J., Barrier, L., and Bouchez, J. (2022b). Li and Si isotopes reveal authigenic clay formation in a palaeo-delta. *Earth Planet. Sci. Lett.*, 578, article no. 117339.